Telomere dysfunction alters the chemotherapeutic profile of transformed cells

Kee-Ho Lee*†, K. Lenhard Rudolph*, Yeun-Jin Ju†, Roger A. Greenberg‡, Linda Cannizzaro§, Lynda Chin*¶, Sarah R. Weiler*, and Ronald A. DePinho*‖**

*Department of Adult Oncology, Dana–Farber Cancer Institute, Departments of ‖Medicine and Genetics, and ¶Dermatology, Harvard Medical School, Boston, MA 02115; †Laboratory of Molecular Oncology, Korea Cancer Center Hospital, Seoul 139-240, Korea; ‡Department of Pathology, Brigham and Women's Hospital, Boston, MA 02115; and §Department of Pathology, Montefiore Medical Center, Albert Einstein College of Medicine, Bronx, NY 10461

Communicated by Frederick W. Alt, Harvard Medical School, Boston, MA, December 28, 2000 (received for review November 9, 2000)

Telomerase inhibition has been touted as a novel cancer-selective therapeutic goal based on the observation of high telomerase levels in most cancers and the importance of telomere maintenance in long-term cellular growth and survival. Here, the impact of telomere dysfunction on chemotherapeutic responses was assessed in normal and neoplastic cells derived from telomerase RNA null (mTERC$^{-/-}$) mice. Telomere dysfunction, rather than telomerase *per se*, was found to be the principal determinant governing chemosensitivity specifically to agents that induced double-stranded DNA breaks (DSB). Enhanced chemosensitivity in telomere dysfunctional cells was linked to therapy-induced fragmentation and multichromosomal fusions, whereas telomerase reconstitution restored genomic integrity and chemoresistance. Loss of p53 function muted the cytotoxic effects of DSB-inducing agents in cells with telomere dysfunction. Together, these results point to the combined use of DSB-inducing agents and telomere maintenance inhibition as an effective anticancer therapeutic approach particularly in cells with intact p53-dependent checkpoint responses.

Major obstacles for anticancer chemotherapy are the cytoxicity of anticancer agents to normal cells as well as tumor cells and the occurrence of resistant tumor cells to chemotherapeutic agents. Therefore, new chemotherapeutic strategies, which could reduce cytotoxicity of normal cells and revert chemoresistance of tumor cells, represent important goals for development of selective cancer therapies. From this view, telomerase is a potential target for selective cancer chemotherapy because most human cancers acquire the ability to activate telomerase and possess shorter telomeres as compared to most normal somatic tissues (1, 2).

The telomerase-deficient mouse is an ideal model system in which to dissect the relative contributions of telomerase activity, telomere function, and tumor suppressors in the response to established chemotherapeutic agents. In the mTERC$^{-/-}$ mouse model, telomere length decreases through serial mTERC$^{-/-}$ intercrosses that produce successive generations (G_1–G_6) of mTERC$^{-/-}$ mice (3, 4). It is only in late (G_4–G_6) mTERC$^{-/-}$ generations that attendant telomere dysfunction (e.g., chromosomal ends with no detectable telomere signals or signal-free ends, aneuploidy, and end-to-end chromosome fusions) leads to widespread proliferative and apoptotic defects (4). Thus, in this model, it is possible to compare the behavior of cells possessing long telomeres and telomerase activity (mTERC$^{+/+}$), long telomeres and no telomerase activity (G_1–G_2 mTERC$^{-/-}$), and short dysfunctional telomeres and no telomerase activity (G_4–G_6 mTERC$^{-/-}$).

The *INK4a* gene produces two distinct gene products, p16^{INK4a} and p19^{ARF}, which are modulators of the pRB and p53 pathways, respectively (5). p16^{INK4a} expression induces a G_1 arrest by inhibiting cyclin-dependent kinases 4 and 6, thus preventing pRB hyperphosphorylation and S phase entry (6). p19^{ARF} interacts with MDM2 and abrogates MDM2-mediated degradation of p53 through the ubiquitin/proteosome pathway (7–10). Although p19^{ARF} has been shown to mediate p53-dependent apoptosis induced by oncogenic stimuli (11–14) and Rb deficiency (7, 15), it is not required for activation of p53 checkpoint function in response to DNA damage (10, 16).

p53 is a key molecular component of the DNA damage response and is a major determinant of the cellular response to chemotherapy and telomere dysfunction (16–19) and plays an important role in mediating the adverse cellular and organismal consequences of telomere dysfunction in normal cells (17, 20). Telomerase activation is perhaps the most common correlate of human cancer and most cancers exhibit loss of p53 or INK4a (1, 21–23). The present study examined the impact of telomere dysfunction on the chemotherapeutic response of transformed cells deficient for p53 or INK4a loci.

Materials and Methods

Generation of Transformed mTERC$^{-/-}$ Mouse Embryo Fibroblasts (MEFs). Mice carrying homozygous deletions of the mouse telomerase RNA gene (*mTERC*), and the INK4a locus or p53 were bred through five or six generations, yielding mice with progressively shorter telomeres with each successive generation, respectively (16–18, 20). MEFs doubly null for *mTERC*, and *INK4a* or *p53* genes were produced from early generation (one mTERC$^{+/+}$INK4a$^{-/-}$ and one G_1 mTERC$^{-/-}$INK4a$^{-/-}$ littermate embryo) and late generation (three G_5 mTERC$^{-/-}$INK4a$^{-/-}$ and three G_6 mTERC$^{-/-}$p53$^{-/-}$ embryos) at day 13.5. The MEFs were transformed by calcium-phosphate cotransfection with Myc/H-RAS^{G12V} plus either mTERC (24) or an empty Bluescript KS(+) (Stratagene) vector as described (18, 20). Single clones were picked and expanded at days 9–13 posttransfection. Telomerase activity of the individual clones was confirmed by the telomeric repeat protocol assay (1). Transformed MEFs were grown in DMEM containing 10% FCS supplemented with penicillin and streptomycin.

Determination of Cell Viability and IC_{50} Value. Transformed clones were plated at a density of 1.0×10^5 cells per well of 6-well plates, grown for 2 days, and treated with the indicated concentrations of doxorubicin, cisplatin, etoposide, and 5-fluorouracil (5-FU). Cell viability was determined by quantitation of the fluorecin-labeled annexin uptake by adherent and floating cell populations (Boehringer Manheim 1828 681) in at least 10,000 cells. For the determination of IC_{50} value, cells were plated in 96-well plates at a density of 7,000 cells per well. The cell viability was monitored 3 days after exposure to doxorubicin, daunorubicin, or actinomycin D by quantification of the conversion of tetra-

Abbreviations: DSB, double-stranded DNA breaks; MEF, mouse embryo fibroblast; 5-FU, 5-fluorouracil; PD, population doubling.

**To whom reprint requests should be addressed. E-mail: ron_depinho@dfci.harvard.edu.

The publication costs of this article were defrayed in part by page charge payment. This article must therefore be hereby marked "*advertisement*" in accordance with 18 U.S.C. §1734 solely to indicate this fact.

solium salt WST-1 into formazan dye (25) (Boeringer Manheim 1644 807), and IC_{50} values were calculated as described (26).

Cytogenetic Analysis. For metaphase preparation, transformed cells were incubated with 0.1 μg/ml colcemid for 1 h and trypsinized single cells were incubated with hypotonic 0.075 M KCl for 20 min, fixed with methanol to acetic acid (3:1 vol/vol), dropped onto frosted microscope slides, and air-dried overnight. The slides were then hybridized to telomere-specific $(CCCTAA)_3$ peptide nucleic acid probe (PerSeptive Biosystems, Framingham, MA), and counterstained with 4′,6-diamidino-2-phenylindole as described (18). Signal-free ends of chromosomes were defined as chromosomal ends with no detectable telomere signal (3, 18). The frequency of chromosomal end-to-end and multichromosomal fusions was determined by counting 10 and 15 metaphases stained with Giemsa per clone, respectively. For all experiments, metaphase preparations of $mTERC^{-/-}$ and mTERC-rescued controls were prepared simultaneously under the same conditions.

Measurement of Telomere Length. Serial passage of individual clones of the transformed MEFs was performed at confluency at a split ratio of 1:16 (corresponding to four population doublings). Telomere length of individual clones was determined at indicated passage numbers by using flow cytometry–fluorescence *in situ* hybridization analysis as described (27). In brief, one million cells were hybridized to a telomere-specific FITC-conjugated $(CCCTAA)_3$ probe (PerSeptive Biosystems). The mean values of flouorescence signals were calculated only for cells in the G_1 fraction as determined by DNA content by flow cytometry.

Results

To assess the effects of telomerase deficiency and telomere dysfunction in modulating responses to chemotherapeutics, initial efforts have focused on INK4a-null cells in which a robust DNA damage response remains operative (16). Because telomerase inhibitors are likely to be administered in conjunction with existing chemotherapeutic drugs, we first examined the response of Myc/RAS-transformed G_5 $mTERC^{-/-}$ $INK4a^{-/-}$ MEFs to a collection of the most commonly used chemotherapeutics in the cancer clinic (19). Mechanistically distinct classes of drugs were selected for analyses, including those acting primarily through intercalation and DSB (doxorubicin), covalent DNA adduct formation (cisplatin), topoisomerase II inhibition (etoposide), and antimetabolite effects (5-FU). Furthermore, to delineate the roles of telomerase and telomere dysfunction in mediating the responses to these chemotherapeutics, the transformed cell lines were generated with cotransfection of either the *mTERC* gene [designated mTERC-rescued or (+mTERC)] or empty vector (designated as +vector). We have shown previously that mTERC transfection leads to reconstitution of telomerase activity and restoration of telomere function (i.e., elimination of signal-free ends and dicentric chromosomes) in late-generation $mTERC^{-/-}$-transformed cells (18, 20).

In the first series of experiments, pools of clonally transformed telomere dysfunctional or mTERC-rescued cultures were exposed to doxorubicin, cisplatin, etoposide, and 5-FU for 24 and 48 h. Significant chemosensitivity was observed only in the telomere dysfunctional population compared to mTERC-rescued counterpart upon exposure to 1 μM doxorubicin (Fig. 1*A*). Specifically, the pooled transformed cell population with telomere dysfunction demonstrated enhanced chemosensitivity to doxorubicin (viability of 40%, open bars) as compared to the mTERC-reconstituted controls (viability of 75%, closed bars; $P < 0.001$). In comparison, reconstitution of mTERC function had little impact on viability of pooled Myc/RAS-transformed cell lines derived from either G_1 $mTERC^{-/-}$ $INK4a^{-/-}$ or

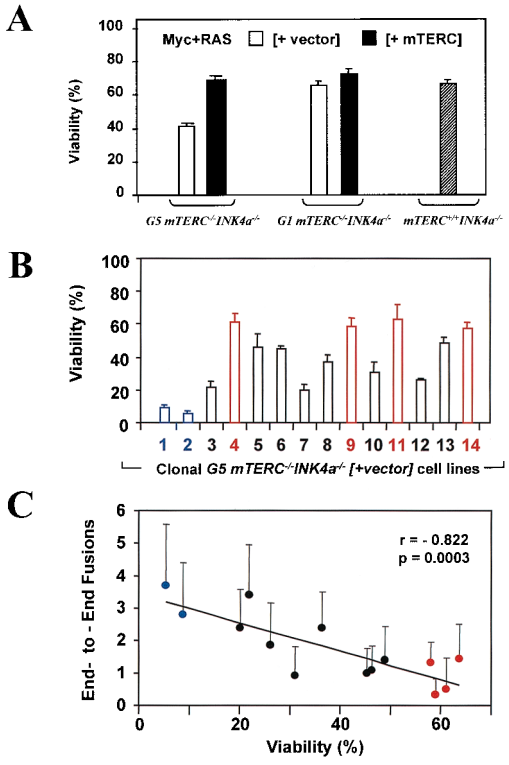

Fig. 1. Chemosensitivity of Myc/RAS-transformed G_5 $mTERC^{-/-}$ $INK4a^{-/-}$ cell lines correlates with the severity of telomere dysfunction. (*A*) Viability of pooled populations of independently derived Myc/RAS-transformed G_5 (n = 14) and G_1 (n = 10) $mTERC^{-/-}$ $INK4a^{-/-}$ clones with (closed bars) and without (opened bars) mTERC-rescued and Myc/RAS-transformed $mTERC^{+/+}$ $INK4a^{-/-}$ cells (n = 10; hatched bars). Cell viability was measured 48 h after continuous exposure to 1 μM doxorubicin in triplicates per experiment. The experiment was repeated several times. Standard deviations were calculated from triplicate assays of one representative experiment. All statistics were calculated by using the INSTAT statistics program (GraphPad, San Diego). (*B*) Chemosensitivity of independently derived Myc/RAS-transformed G_5 $mTERC^{-/-}$ $INK4a^{-/-}$ clonal cell lines 48 h after continuous exposure to 1 μM doxorubicin. (*C*) The degree of pretreatment telomere dysfunction, as measured by number of Robertsonian end-to-end fusions, correlates with chemosensitivity to doxorubicin, as determined by viability at 48 h after exposure to 1 μM doxorubicin. Fifteen metaphases per clone were analyzed and mean numbers of chromosomal end-to-end fusion were plotted against percentage viability. SDs were calculated from fusion counts of 15 metaphases from each clone.

$mTERC^{+/+}$ $INK4a^{-/-}$ controls upon exposure to the same treatment protocol (Fig. 1*A*). Similarly, functional status of the telomeres did not impact on chemosensitivity of G_5 $mTERC^{-/-}$ $INK4a^{-/-}$ cells upon exposure to cisplatin, etoposide, and 5-FU (data not shown). The selective rescue by mTERC in late-generation-transformed $mTERC^{-/-}$ $INK4a^{-/-}$ cells with documented telomere dysfunction, but not in early-generation-transformed $mTERC^{-/-}$ $INK4a^{-/-}$ controls, indicates that telomere dysfunction, rather than telomerase deficiency *per se*, is the major parameter governing sensitivity to doxorubicin.

Taking advantage of the inherent heterogeneity in telomere length (hence telomere functional status) among independently derived clones from parental MEF cultures, we further correlated the degree of doxorubicin chemosensitivity with the severity of telomere dysfunction by measuring the cytotoxic response for each Myc/RAS-transformed G_5 $mTERC^{-/-}$ $INK4a^{-/-}$ clonal cell line (n = 14). As with the pooled population studies above, percentage viability was determined after 48 h of continuous exposure to 1 μM doxorubicin. Although baseline viability of all independently derived clones in normal

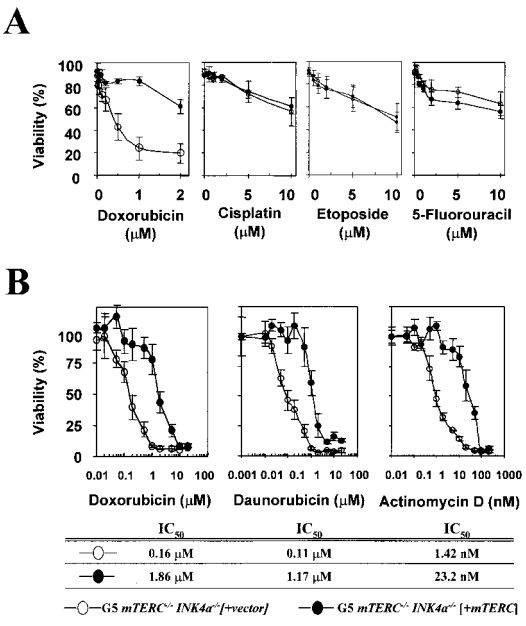

Fig. 2. Loss of telomere function increases chemosensitivity toward DSB-inducing agents. (*A*) Dose–response curves of early passage [population doubling (PD) 20–40] Myc/RAS-transformed G_5 mTERC$^{-/-}$ INK4a$^{-/-}$ cells (○) and mTERC-rescued controls (●) determined 24 h after continuous exposure to the indicated concentrations of different anticancer agents. (*B*) Dose–response curves and IC_{50} values of early passage (PD 20–40) Myc/RAS-transformed G_5 mTERC$^{-/-}$ INK4a$^{-/-}$ MEFs (○) and mTERC-rescued controls (●) in response to continuous exposure to different members of DSB-inducing agents (19). Each data point represents the mean of triplicate assays performed with either mixture of two telomere dysfunctional mTERC$^{-/-}$ INK4a$^{-/-}$-transformed cell lines (○, representing clones 1 and 2 from Fig. 1*B*), or mixture of two telomere functional mTERC-rescued INK4a$^{-/-}$-transformed cell lines (●). All four independently derived transformed cell lines in this experiment were derived from Myc/RAS transformation of the same parental MEF culture. SDs were calculated from triplicate assays for each data point from a representative experiment. All statistics were calculated by using the INSTAT statistics program.

media without doxorubicin was comparable, the level of doxorubicin sensitivity was highly variable among these transformed G_5 mTERC$^{-/-}$ INK4a$^{-/-}$cell lines (Fig. 1*B*). In sharp contrast, clonal-transformed cells with functional telomeres exhibited a more uniform level of sensitivity that reflected their enhanced viability upon exposure to doxorubicin (data not shown). To provide a molecular basis for the broad range of chemosensitivity observed among the G_5 mTERC$^{-/-}$ INK4a$^{-/-}$ clones shown in Fig. 2*B*, the degree of telomere dysfunction was determined in the pretreatment cultures by quantifying the frequency of end-to-end fusions and signal-free ends, both steadfast correlates of telomere dysfunction in mouse cells wild type for p53 (3, 4, 18). As shown in Fig. 1*C*, the baseline degree of telomere dysfunction proved to be a strong predictor of the chemosensitivity to doxorubicin in these transformed cells ($P = 0.0003$). For example, the highly doxorubicin-sensitive clones 1 and 2 (blue bars in Fig. 1*B*) were found to be highly fusigenic, harboring a total of 42 and 56 fusions in 15 metaphases, respectively (mean of 2.8 and 3.8 fusions per metaphase, see blue circles in Fig. 1*C*). In comparison, the relatively resistant clones 4, 9, 11, and 14 (red bars in Fig. 1*B*) possessed only 8, 5, 21, and 20 fusions in 15 metaphases, respectively (means of 0.5, 0.33, 1.46, and 1.34 fusions per metaphase, see red circles in Fig. 1*C*). These results reinforce the view that the link between telomerase deficiency and doxorubicin sensitivity relates largely to the degree of telomere dysfunction.

Next, we sought to better characterize this specific chemosensitivity to doxorubicin in telomere dysfunctional cells. To this end, we measured the dose responses of two telomere dysfunctional clones 1 and 2 (see Fig. 1*B*) to varying concentration of doxurubicin, cisplatin etoposide, and 5-FU and compared them to that of two mTERC-reconstituted controls (Fig. 2*A*). Consistent with data obtained from pooled population studies in Fig. 1, continuous exposure (24 h) to doxorubicin alone was found to exert a profound cytotoxic effect against the transformed cell lines possessing short dysfunctional telomeres (Fig. 2*A*, ○). Interestingly, increased death of Myc/RAS-transformed G_5 mTERC$^{-/-}$ INK4a$^{-/-}$ cells in response to cisplatin was seen only after prolonged continuous exposure (10 days, data not shown), in line with the delayed accumulation of DSBs by formation of platinum-DNA adducts induced by cisplatin (19). This sensitivity to doxorubicin was markedly attenuated in mTERC-rescued cell lines (Fig. 2*A*, ●). Detailed cytogenetic analyses confirmed restoration of telomere function in the mTERC-rescued cell lines as manifested by normalization of cytogenetics and presence of telomere signal at all termini (data not shown and see ref. 18), whereas the cell lines without mTERC reconstitution (○) lacked telomerase activity and exhibited significant telomere dysfunction (see below).

The enhanced sensitivity to doxorubicin and the lack of significant cytotoxic differences with other classes of chemotherapeutic agents implied cytotoxic synergy between telomere dysfunction and agents possessing efficient DSB activity. Although etoposide possess DSB activity via its ability to inhibit topoisomerase II (28), it is well-known that topoisomerase II inhibitors have different clinical potencies and activity spectra. Specifically, at the therapeutic dosages used in these studies (which is comparable to 1 μg/ml or 1.7 μM achievable in patient sera clinically) (28), etoposide is known to induce 3–20 times more efficiently topoisomerase II-mediated single-stranded breaks, than topoisomerase II-mediated double-stranded breaks (28, 29). On the other hand, doxorubicin (30–33), daunorubicin (30, 31), and actinomycin D (32, 33) produce almost exclusively double-stranded breaks. To substantiate this interaction, we demonstrated that these mechanistically related compounds indeed produced similarly potent cytotoxic effects in the setting of telomere dysfunction (Fig. 2*B*). Notably, mTERC-rescued counterparts exhibited a >10-fold increase in IC_{50} values for each compound, a finding of clinical significance in light of the extremely narrow therapeutic indices of these agents in humans. Together, these results demonstrated specific and potent cytotoxic synergy between telomere dysfunction and doxorubicin or related DSB-inducing compounds.

The basis for the cytotoxic synergy between telomere dysfunction and doxorubicin was examined by conducting cytogenetic analyses on doxorubicin-treated transformed G_5 mTERC$^{-/-}$ INK4a$^{-/-}$ cells and mTERC-rescued controls. After 48 h of continuous doxorubicin exposure at various dosages, both G_5 mTERC$^{-/-}$ INK4a$^{-/-}$-transformed cells and corresponding mTERC-rescued cells exhibit increased p arm fusions compared to pretreatment baseline level (data not shown). However, only transformed G_5 mTERC$^{-/-}$ INK4a$^{-/-}$ clones incurred severe chromosomal fragmentation (data not shown) as well as widespread multichromosomal fusions engaging both p and q arm termini (Fig. 3 *A* and *B*). Although doxorubicin-mediated increase in p arm fusions and DSBs were observed, transformed mTERC-rescued G_5 mTERC+ INK4a$^{-/-}$ clones (as well as transformed mTERC$^{+/+}$ INK4a$^{-/-}$ and G_1 mTERC$^{-/-}$ INK4a$^{-/-}$, and their mTERC-rescued counterparts) exhibited a low number of multichromosomal fusions (Fig. 3 *A* and *B*; data not shown for mTERC$^{+/+}$ and G_1 mTERC$^{-/-}$). Specifically, G_5 mTERC$^{-/-}$ INK4a$^{-/-}$ clones exhibited an average of 5.13 multichromosomal fusions per metaphase compared to 0.27 multichromosomal fusions per metaphase in the mTERC-rescued

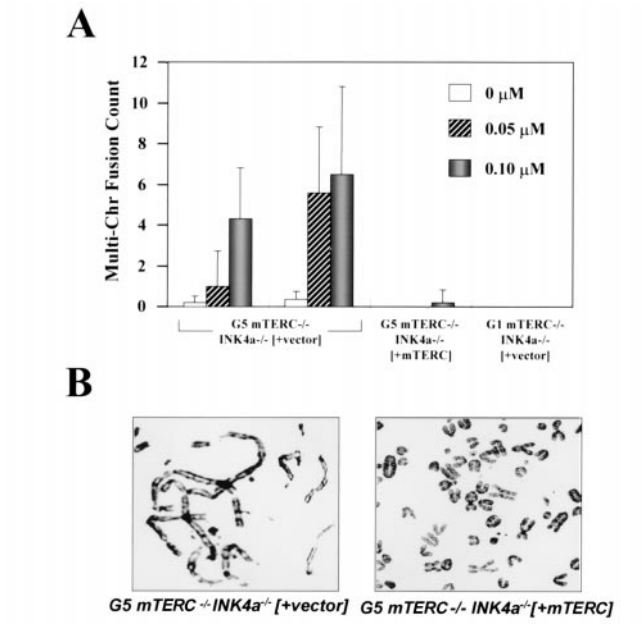

Fig. 3. Multichromosomal fusions are induced in cells with dysfunctional telomeres in response to doxorubicin. (*A*) The incidence of multichromosomal fusions in response to 48 h of continuous exposure to doxorubicin at the indicated concentrations. Lower dosages of doxorubicin were used in this experiment because significant cell death and cell cycle arrest at higher concentrations (>0.1 μM) did not allow for the preparation of metaphases. Ten metaphases were analyzed for each experimental point and mean multichromosomal fusion counts were plotted. Significant incidence of multichromosomal fusions was seen only in G_5 mTERC$^{-/-}$ INK4a$^{-/-}$-transformed cells, a correlate of enhanced sensitivity of these cells to doxorubicin. (*B*) Representative metaphase spreads obtained at 48 h after continuous exposure to 0.1 μM doxorubicin, showing multichromosomal fusions in G_5 mTERC$^{-/-}$ INK4a$^{-/-}$-transformed MEFs but not in mTERC-rescued controls.

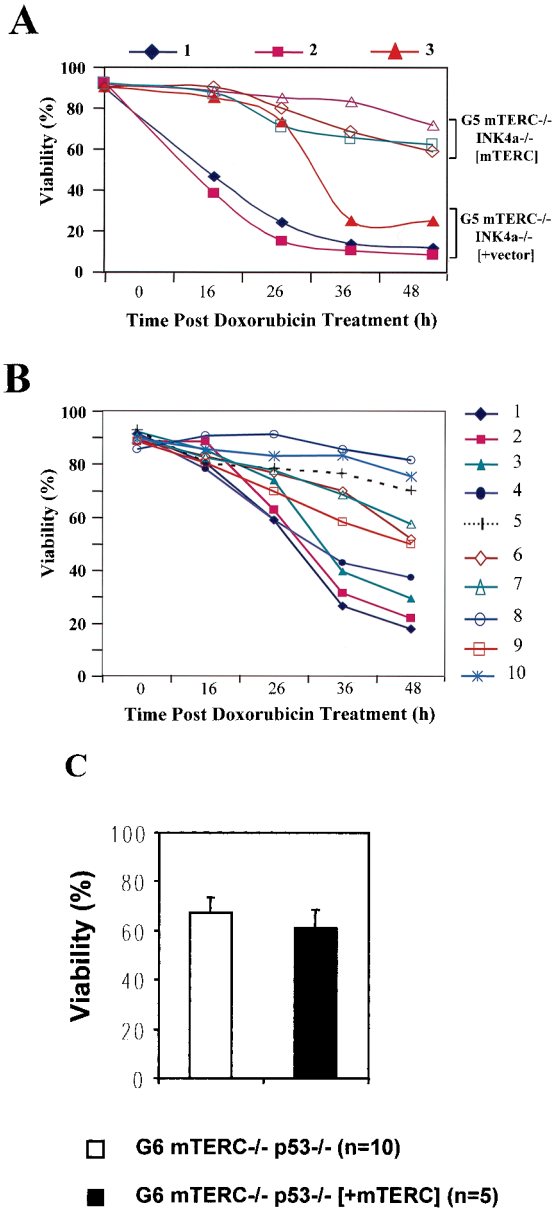

Fig. 4. p53 is a critical modulator of doxorubicin chemosensitivity induced by telomere dysfunction. (*A*) Kinetics of viability loss observed in early passaged (PD 20–40) Myc/RAS-transformed G_5 mTERC$^{-/-}$ INK4a$^{-/-}$ cells with (open symbols, $n = 3$) and without (closed symbols, clones 1–3 corresponding to clones 1–3 in Fig. 1*B*) mTERC reconstitution, measured for 48 h of continuous exposure to doxorubicin (1 μM). Note, clone 3 with mutant p53 exhibited a delayed kinetics compared to clones 1 and 2. (*B*) Kinetics of viability loss observed for each of 10 individual Myc/RAS-transformed G6 mTERC$^{-/-}$ p53$^{-/-}$ clones at early passage (PD 20–40), measured for 48 h of continuous exposure to doxorubicin (1 μM). (*C*) Viability of pooled populations of independently derived Myc/RAS-transformed G_6 mTERC$^{-/-}$ p53$^{-/-}$ clones with (closed bars, $n = 5$) and without (opened bars, $n = 10$) mTERC-rescue. Cell viability was measured 48 h after continuous exposure to 1 μM doxorubicin.

counterparts ($P < 0.001$). Moreover, we have observed that, in treated cultures carried for 1-mo duration, there were no multichromosomal fusions in any of the surviving cells irrespective of telomerase status. These observations suggest that although cells may survive with p arm fusions, multichromosomal fusions lead to cell death. Thus, the cytogenetic finding of multichromosomal fusions correlates with chemosensitivity to doxorubicin in this system. In contrast, prolonged 5-FU treatment in these cultures generated negligible level of multichromosomal fusions regardless of telomerase or telomere status (data not shown), correlating to the lack of specific sensitivity to this chemotherapeutic agent. Together, the observation of multichromosomal fusions may be a reflection of both availability and accessibility of telomere-free ends in the presence of doxorubicin-generated DSBs.

Next, we performed serial doxorubicin cytotoxicity determinations over time for G_5 mTERC$^{-/-}$ INK4a$^{-/-}$-transformed cell lines with and without mTERC reconstitution. mTERC-rescued clones maintained viability throughout the 48-h exposure, whereas vector-transduced clones exhibited a marked and rapid decline (Fig. 4*A*, compare open symbols to closed symbols; clones 1, 2, and 3 correspond to clones in Fig. 1*B*). One vector-transduced cell line (clone 3) exhibited an unusual profile of delayed onset of cytotoxicity at 24 h and eventually displayed a level of cytotoxicity comparable to clones 1 and 2. Molecular characterization revealed that unlike the other five clones depicted in Fig. 4*A*, clone 3 harbored high basal level of p53 protein. Upon treatment with doxorubicin, all except clone 3 exhibited stabilization of p53 protein as well as induction of its transcriptional target p21. Thus, clone 3 with the unusual cytotoxicity profile has sustained somatic inactivation of p53.

The altered cytotoxicity profile of clone 3 and the known role of p53 in governing the response to a broad spectrum of chemotherapeutics (34–37) prompted a more direct assessment of how p53 status impacts on the doxorubicin response of telomere dysfunctional cells. To this end, we generated 10 Myc/RAS-transformed

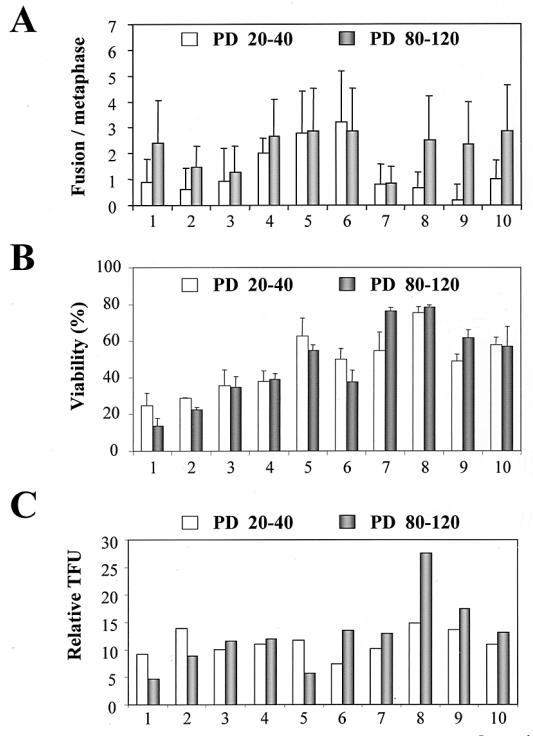

Fig. 5. Telomere dysfunction, telomere length, and viability of p53-deficient cells as a function of passage. (*A*) The degree of pretreatment telomere dysfunction, as measured by number of chromosomal end-to-end fusions in early (PD 20–40) and late passages (PD 80–120) of 10 independently derived mTERC$^{-/-}$ p53$^{-/-}$-transformed clones. Fifteen metaphases per clone were analyzed. (*B*) Viability of early and late passaged mTERC$^{-/-}$ p53$^{-/-}$-transformed clones after 48 h of continuous exposure to 1 μM doxorubicin. (*C*) Flow–fluorescence *in situ* hybridization determination of telomere lengths in early and late passaged mTERC$^{-/-}$ p53$^{-/-}$-transformed clones.

G_6 mTERC$^{-/-}$ p53$^{-/-}$ MEF cell lines and characterized their doxorubicin sensitivity. Most notably, unlike the transformed G_5 mTERC$^{-/-}$ INK4a$^{-/-}$ cell lines in which significant cell death was evident as early as 16 h after treatment, doxorubicin cytotoxicity was not observed in transformed G_6 mTERC$^{-/-}$ p53$^{-/-}$ clones until 36 h, similar to the G_5 mTERC$^{-/-}$ INK4a$^{-/-}$ clone 3 mutant for p53 (Fig. 4 *A* and *B*). Moreover, mTERC reconstitution did not alter the viability of pooled transformed G_6 mTERC$^{-/-}$ p53$^{-/-}$ cells to doxorubicin unlike G_5 mTERC$^{-/-}$ INK4a$^{-/-}$ cell lines (Fig. 4*C* and compare to Fig. 1*A*), despite documented comparable level of telomere dysfunction (1.53 vs. 1.76 fusion per metaphase, respectively, Fig. 5*A*, open bars). The differential rescue of cytotoxic profiles by mTERC reconstitution in G_5 mTERC$^{-/-}$ INK4a$^{-/-}$ but not in G_6 mTERC$^{-/-}$ p53$^{-/-}$ cells pointed to p53 as a critical modulator of increased chemosensitivity induced by telomere dysfunction.

The capacity of p53 deficiency to mute the cytotoxic response in the setting of telomere dysfunction prompted us to ask whether additional telomere shortening, brought about by extensive passage in culture, would further sensitize transformed G_6 mTERC$^{-/-}$ p53$^{-/-}$ cells to doxorubicin. To this end, all 10 independently derived G_6 mTERC$^{-/-}$ p53$^{-/-}$ clones were passaged in culture for up to 120 population doublings and monitored for telomere dysfunction, telomere length, and chemosensitivity (Fig. 5). These passaged G_6 mTERC$^{-/-}$p53$^{-/-}$ clones did not exhibit an increased chemosensitivity as a function of passage, despite increasing severity of telomere dysfunction in some clones (Fig. 5 *A* and *B*). Moreover, flow cytometry fluorescence *in situ* hybridization telomere length determinations of early vs. late passaged clones revealed similar or increased telomere signals in 7 of 10 cell lines tested (Fig. 5*C*), raising the possibility of telomerase-independent mechanism for telomere length maintenance that may contribute to chemoresistance in these p53 mutant cells. Such telomerase-independent mechanism, so-called ALT, have been documented in mammalian cells (38, 39).

Discussion

The observation that most cancers express high levels of telomerase (1) and telomere maintenance is required for long-term cellular growth and survival (4, 20, 40, 41) supports the basis of a telomerase inhibitor as a novel cancer-selective therapeutic. This report uncovers a link between telomere dysfunction and chemosensitivity specifically toward agents that induce DSBs. The enhanced chemotoxicity was observed in Myc/RAS-transformed MEFs derived from G_5 mTERC$^{-/-}$ INK4a$^{-/-}$ mice as compared to G1 mTERC$^{-/-}$ INK4a$^{-/-}$ or G_5 mTERC$^{-/-}$ INK4a$^{-/-}$ cells reconstituted with mTERC exposed to doxorubicin and other related compounds. Furthermore, within MEF cultures of transformed G_5 mTERC$^{-/-}$ INK4a$^{-/-}$ cells, there were subclones containing critically shortened and dysfunctional telomeres that were highly sensitive and others that were resistant or less sensitive possessing less dysfunctional telomeres. This variation among individual clones established a strong positive correlation between telomere dysfunction and chemosensitivity and further pointed to telomere dysfunction, rather than telomerase activity status, as the principle determinant of chemosensitivity to DSB agents.

Notably, chemosensitivity of transformed G_5 TERC$^{-/-}$ INK4a$^{-/-}$ cells was muted in cells deficient for p53 (Fig. 4*A*). Recent publications (17, 20) have identified p53 as a crucial downstream mediator in response to dysfunctional telomeres. The present results together with the previous findings raise the possibility that loss of p53 function might facilitate the activation of resistance mechanisms designed to cope with DSBs in the setting of telomere dysfunction. Such mechanism could include an increase in homologous recombination and/or nonhomologous end-joining activity, activation of recombination-mediated telomere maintenance (i.e., the ALT mechanism), among others. At present, the mechanistic basis for how p53 deficiency mutes the cytotoxic response in telomere dysfunctional cells remains to be determined. Because flow–fluorescence *in situ* hybridization telomere length determinations reveal unchanged or increased telomere signal in 7 of 10 cell lines tested (Fig. 5*C*), one possibility is that p53 deficiency might play a permissive role in the activation of a telomerase-independent telomere maintenance mechanism, a process that may be facilitated by the known higher levels of homologous recombination activity in ALT cells (42) and cells lacking p53 (43, 44). Along these lines, it is notable that human ALT tumor cell lines are often p53 defective (38, 39). Further studies will be necessary to determine the relative contributions of loss of p53 checkpoints vs. a lower threshold for activation of ALT in p53-null telomere dysfunctional cells.

An important consideration of a combined antitelomerase and chemotherapy regime will be the impact on normal cells. Previously, our reports have demonstrated that telomere shortening in mTERC$^{-/-}$ mice decreases the capacity to cope with various stresses such as wound healing and blood cell depletion, especially in aged animals (45). Thus, a potential elevation of hematotoxic side effects of chemotherapeutics when combined with telomere inhibitors should be a prominent consideration as clinical trials move forward. The additional risk of developing secondary malignancies in response to telomere shortening and genetic instability as seen in aged mTERC$^{-/-}$ mice (45) also has to be considered, particularly in the setting of p53 mutant tumors. That p53 deficiency may also attenuate the therapeutic impact of a doxorubicin/antitelomerase regimen via the activa-

tion of adaptive mechanisms presage the need to identify and neutralize such mechanisms to maximize the clinical impact of this novel regimen. By the same token, activation of any telomerase-independent mechanism for telomere maintenance in the setting of antitelomerase therapy would diminish the synergy of such a treatment regimen. Against this backdrop, although a critical and careful evaluation of telomere inhibitors in cancer therapies is certainly required, our present data indicate that the inhibition of telomere maintenance will act to chemosensitize cancers to doxorubicin and related compounds and, thus, encourage the development and evaluation of this therapeutic combined option.

We thank G. Merlino, C. Greider, S. Artandi, N. Sharpless, K.-K. Wong, S. Johnson, and S. Chang for critical reading of the manuscript. K.H.L. is supported by a grant from National Nuclear R & D program, Korean Ministry of Science and Technology. K.L.R. is supported by the Deutsche Forschungsgemeinschaft (Ru 745/1–1). L.C. is supported by National Institutes of Health Grant K08AR02104–01 and is a V Foundation Scholar. R.A.G. was supported by National Institutes of Health Training Grant 5T32GM07491. The work was supported by grants from the National Institutes of Health (R01HD34880; R01HD28317) and an American Heart Association grant-in-aid (to R.A.D.). R.A.D is an American Cancer Society Research Professor and recipient of the Steven and Michele Kirsch Foundation Investigator Award. Support from the Dana Farber Cancer Institute Cancer Core grant to R.A.D. and L.C. is acknowledged.

1. Kim, N. W., Piatyszek, M. A., Prowse, K. R., Harley, C. B., West, M. D., Ho, P. L., Coviello, G. M., Wright, W. E., Weinrich, S. L. & Shay, J. W. (1994) *Science* **266,** 2011–2015.
2. Nakamura, T. M., Morin, G. B., Chapman, K. B., Weinrich, S. L., Andrews, W. H., Lingner, J., Harley, C. B. & Cech, T. R. (1997) *Science* **277,** 955–959.
3. Blasco, M. A., Lee, H. W., Hande, M. P., Samper, E., Lansdorp, P. M., DePinho, R. A. & Greider, C. W. (1997) *Cell* **91,** 25–34.
4. Lee, H. W., Blasco, M. A., Gottlieb, G. J., Horner, J. W., Greider, C. W. & DePinho, R. A. (1998) *Nature (London)* **392,** 569–574.
5. Sherr, C. J. (1998) *Genes Dev.* **12,** 2984–2991.
6. Serrano, M., Hannon, G. J. & Beach, D. (1993) *Nature (London)* **366,** 704–707.
7. Pomerantz, J., Schreiber-Agus, N., Liegeois, N. J., Silverman, A., Alland, L., Chin, L., Potes, J., Orlow, I., Lee, H. W., Cordon-Cardo, C. & DePinho, R. A. (1998) *Cell* **92,** 713–723.
8. Zhang, Y., Xiong, Y. & Yarbrough, W. G. (1998) *Cell* **92,** 725–734.
9. Kamijo, T., Weber, J. D., Zambetti, G., Zindy, F., Roussel, M. F. & Sherr, C. J. (1998) *Proc. Natl. Acad. Sci. USA* **95,** 8292–8297.
10. Stott, F. J., Bates, S., James, M. C., McConnell, B. B., Starborg, M., Brookes, S., Palmero, I., Ryan, K., Hara, E., Vousden, K. H. & Peters, G. (1998) *EMBO J.* **17,** 5001–5014.
11. de Stanchina, E., McCurrach, M. E., Zindy, F., Shieh, S. Y., Ferbeyre, G., Samuelson, A. V., Prives, C., Roussel, M. F., Sherr, C. J. & Lowe, S. W. (1998) *Genes Dev.* **12,** 2434–2442.
12. Palmero, I., Pantoja, C. & Serrano, M. (1998) *Nature (London)* **395,** 125–126.
13. Zindy, F., Eischen, C. M., Randle, D. H., Kamijo, T., Cleveland, J. L., Sherr, C. J. & Roussel, M. F. (1998) *Genes Dev.* **12,** 2424–2433.
14. Radfar, A., Unnikrishnan, I., Lee, H. W., DePinho, R. A. & Rosenberg, N. (1998) *Proc. Natl. Acad. Sci. USA* **95,** 13194–13199.
15. Bates, S., Phillips, A. C., Clark, P. A., Stott, F., Peters, G., Ludwig, R. L. & Vousden, K. H. (1998) *Nature (London)* **395,** 124–125.
16. Kamijo, T., Zindy, F., Roussel, M. F., Quelle, D. E., Downing, J. R., Ashmun, R. A., Grosveld, G. & Sherr, C. J. (1997) *Cell* **91,** 649–659.
17. Karlseder, J., Broccoli, D., Dai, Y., Hardy, S. & de Lange, T. (1999) *Science* **283,** 1321–1325.
18. Greenberg, R. A., Chin, L., Femino, A., Lee, K. H., Gottlieb, G. J., Singer, R. H., Greider, C. W. & DePinho, R. A. (1999) *Cell* **97,** 515–525.
19. Teicher, B. A., O'Dwyer, P. J., Johnson, S. W., Hamilton, T. C., Allegra, C. J., Grem, J. L., Stewart, C. F. & Ratain, M. J. (1997) in *Cancer Principles and Practices* of *Oncology*, eds. DeVita, V. T., Jr., Rosenberg, S. A. & Hellman, S. (Lippincott–Raven, New York), 5th Ed., pp. 405–467.
20. Chin, L., Artandi, S. E., Shen, Q., Tam, A., Lee, S. L., Gottlieb, G. J., Greider, C. W. & DePinho, R. A. (1999) *Cell* **97,** 527–538.
21. Hollstein, M., Sidransky, D., Vogelstein, B. & Harris, C. C. (1991) *Science* **253,** 49–53.
22. Frebourg, T. & Friend, S. H. (1993) *J. Natl. Cancer Inst.* **85,** 1554–1557.
23. Liggett, W. H., Jr. & Sidransky, D. (1998) *J. Clin. Oncol.* **16,** 1197–1206.
24. Blasco, M. A., Funk, W., Villeponteau, B. & Greider, C. W. (1995) *Science* **269,** 1267–1270.
25. Liu, S. Q., Saijo, K., Todoroki, T. & Ohno, T. (1995) *Nat. Med.* **1,** 267–271.
26. Chou, J. & Chou, T.-C. (1985) *Dose-Effect Analysis with Microcomputers: Quantitation of ED50, LD50, Synergism, Antagonism, Low-Dose Risk, Receptor Ligand Binding and Enzyme Kinetics* (Elsevier-BioSoft, Cambridge, U.K.).
27. Rufer, N., Dragowska, W., Thornbury, G., Roosnek, E. & Lansdorp, P. M. (1998) *Nat. Biotechnol.* **16,** 743–747.
28. Pommier, Y., Fesen, M. R. & Goldwasser, F. (1996) in *Cancer Chemotherapy and Biotherapy*, eds. Chabner, B. A. & Longo, D. L. (Lippincott–Raven, New York), pp. 435–461.
29. Long, B. H., Musial, S. T. & Brattain, M. G. (1985) *Cancer Res.* **45,** 3106–3112.
30. Binaschi, M., Capranico, G., Dal, B. L. & Zunino, F. (1997) *Mol. Pharmacol.* **51,** 1053–1059.
31. Doroshow, J. H. (1996) in *Cancer Chemotherapy and Biotherapy*, eds. Chabner, B. A. & Longo, D. L. (Lippincott-Raven, New York), pp. 409–434.
32. Zwelling, L. A., Kerrigan, D. & Michaels, S. (1982) *Cancer Res.* **42,** 2687–91.
33. Ross, W. E. & Bradley, M. O. (1981) *Biochim. Biophys. Acta* **654,** 129–134.
34. Lee, J. M. & Bernstein, A. (1993) *Proc. Natl. Acad. Sci. USA* **90,** 5742–5746.
35. Lowe, S. W., Ruley, H. E., Jacks, T. & Housman, D. E. (1993) *Cell* **74,** 957–967.
36. el Rouby, S., Thomas, A., Costin, D., Rosenberg, C. R., Potmesil, M., Silber, R. & Newcomb, E. W. (1993) *Blood* **82,** 3452–3459.
37. Lowe, S. W., Bodis, S., McClatchey, A., Remington, L., Ruley, H. E., Fisher, D. E., Housman, D. E. & Jacks, T. (1994) *Science* **266,** 807–810.
38. Bryan, T. M., Englezou, A., Gupta, J., Bacchetti, S. & Reddel, R. R. (1995) *EMBO J.* **14,** 4240–4248.
39. Bryan, T. M., Englezou, A., Dalla-Pozza, L., Dunham, M. A. & Reddel, R. R. (1997) *Nat. Med.* **3,** 1271–1274.
40. Bodnar, A. G., Ouellette, M., Frolkis, M., Holt, S. E., Chiu, C. P., Morin, G. B., Harley, C. B., Shay, J. W., Lichtsteiner, S. & Wright, W. E. (1998) *Science* **279,** 349–352.
41. Vaziri, H. & Benchimol, S. (1998) *Curr. Biol.* **8,** 279–282.
42. Dunham, M. A., Neumann, A. A., Fasching, C. L. & Reddel, R. R. (2000) *Nat. Genet.* **26,** 447–450.
43. Mekeel, K. L., Tang, W., Kachnic, L. A., Luo, C. M., DeFrank, J. S. & Powell, S. N. (1997) *Oncogene* **14,** 1847–1857.
44. Sturzbecher, H. W., Donzelmann, B., Henning, W., Knippschild, U. & Buchhop, S. (1996) *EMBO J.* **15,** 1992–2002.
45. Rudolph, K. L., Chang, S., Lee, H. W., Blasco, M., Gottlieb, G. J., Greider, C. & DePinho, R. A. (1999) *Cell* **96,** 701–712.